Simulation of misfit dislocation loops at the Ag/Cu(111) interface

Torben Rasmussen
Theoretical Division, Los Alamos National Laboratory, New Mexico 87545, USA
(May 24, 2000)

Molecular Dynamics simulations combined with the Nudged Elastic Band Method for finding transition states and corresponding activation energies are used to study mechanisms of nucleation, growth, and motion of misfit dislocation loops at the Ag/Cu(111) interface. A variety of mechanisms involving concerted motion of several atoms are identified. Nucleation has the highest activation energy, ~ 1 eV. Growth and motion of the loops have activation energies in the range 0.3 - 0.7 eV.

Recent years' applications of scanning tunnelling microscopy (STM) in conjunction with atomic scale modelling have led to rather intriguing findings concerning surface/interface structures in studies of metal on metal growth, in particular for systems with a large lattice constant mismatch [1–5]. In the case of Au deposited on Ni(111) a combined STM/atomistic study [1] found that two distinct interface structures exist. When a single monolayer (ML) of Au is deposited on Ni(111) at 170 K and subsequently imaged at room temperature (RT) by STM, an incommensurable Moiré structure is observed. The Moiré structure can be described as a slightly compressed (n-1)$\times$(n-1) hexagonal Au layer positioned ontop an n $\times$ n Ni(111) substrate, with n = 9 or 10. If Au is deposited at RT or if the Moiré structure is annealed to 400 K a two dimensional periodic array of misfit dislocations is formed in the topmost Ni layer. The period is 9.7 $\times$ 9.7 with respect to the Ni substrate periodicity. The misfit dislocations are imaged by STM as triangular depressions of side length 3, 4, 5, or 6 atoms in the Au overlayer surrounding small triangular clusters consisting of 0, 1, 3, or 6 protruding atoms, respectively. All Au atoms are in perfect (111)–registry except for a slightly decreased lattice parameter and the vertical displacements at the triangles. When Ag is deposited on Cu(111) very analogous behavior to Au/Ni(111) is observed. After deposition of roughly 1 ML of Ag on Cu(111) at RT a periodic array of triangular misfit dislocations is observed by STM [2,3]. The period of the superstructure is 9.43 $\times$ 9.43 with respect to the underlying Cu substrate periodicity [3].

The misfit dislocations form [1,4] by expelling a row of nearest neighbor atoms from the topmost substrate layer. Removal of, e.g., a row of 4 atoms from the substrate allows a 6–atom triangle of side length 3 to shift from fcc postions to hcp positions thus forming a misfit loop surrounding the displaced triangle. The imprint of this loop is imaged by STM as a triangular depression in the overlayer of side length 4 surrounding 1 protruding atom. The shift of the 6–atom triangle allows the overlayer atoms to coordinate to 3 or 4 substrate atoms in contrast to the Moiré structure where some atoms are positioned in energetically unfavorable atop sites. The previous atomistic studies of misfit loops [1,4] focused on the energetics of the two different equilibrium structures,

	Ag	Cu
a_0 (Å)	4.054	3.585
C_{44} (GPa)	50.4 (51.1)[a]	81.5 (81.8)[a]
C_{11} (GPa)	130.5 (131.5)[a]	175.8 (176.2)[a]
C_{12} (GPa)	97.9 (97.3)[a]	125.6 (124.9)[a]
B (GPa)	108.8 (108.7)[a]	142.0 (142.0)[a]
γ_{isf} (mJ/m^2)	24.7 (21-29)[b]	52.5 (51-53)[b]
γ_{us} (mJ/m^2)	111	169
γ_{111} (mJ/m^2)	738 (1172)[c]	1198 (1952)[c]
γ_{100} (mJ/m^2)	814 (1200)[c]	1291 (2166)[c]
E_v (eV)	1.05 ($\simeq$ 1.1)[d]	1.32 ($\simeq$ 1.3)[d]
Heat of Sol. (eV)	0.38 (0.39)[e]	0.24 (0.25)[e]

[a] Ref. [12]; [b] Ref. [13]; [c] Ref. [14]; [d] Ref. [15]; [e] Ref. [16].

TABLE I. Zero temperature values for lattice constants, elastic constants, relaxed planar defects, relaxed vacancy formation energies, and heats of solution for Ag and Cu obtained with the EMT potentials used in this work. γ_{isf} is the intrinsic stacking–fault energy and γ_{us} is the fcc $\rightarrow$ hcp unstable stacking energy. The heat of solution entry under Ag is for Ag in Cu and similarily for the Cu entry. Reference experimental and *ab initio* results are given in parentheses.

but neither provided insight into actual mechanisms or activation barriers pertinent to formation of misfit loops, which could be important for the understanding of metal on metal growth and the properties of, e.g., multilayered thin films.

It is the aim of the present work to provide such insight by investigating nucleation, growth, and motion of misfit dislocation loops by atomistic simulation. The atomic interactions are described by *effective–medium theory* (EMT) [6,7] many–body potentials. A new parameterization [8] of EMT for Cu and Ag was developed which reproduces properties such as elastic constants, relaxed vacancy formation energies and intrinsic stacking–fault energies, and heats of solutions very well, see table I. As usually with effective–medium–like potentials, such as EMT or *embedded atom method* (EAM) potentials, free–surface energies (γ_{111} and γ_{100}) tend to be underestimated. The simulations aim at mimicing an experimental anneal of the low temperature Moiré structure. Hence, the approach, taken here, is to perform Molec-

ular Dynamics (MD) simulations at elevated temperatures, identify transitions, and find the transition paths and activation energies associated with those transitions. For the latter purpose the *nudged elastic band* (NEB) method [9] is used. The simulations are carried out as MD simulations of isolated Ag islands on wide Cu(111) substrates or as simulations of 1 supercell ($n_{Cu} = 9$ or 10) or 4 supercells ($n_{Cu} = 19; n_{Ag} = 17$) with in–plane periodic boundary conditions. The substrates consists of 3 fixed (111) layers and 4 (111) layers where the atoms are allowed to move. The temperature is varied in the range $500 - 800\,\mathrm{K}$ using Langevin dynamics [10] with a time step of $5 \times 10^{-15}\,\mathrm{s}$.

Experimentally, triangular misfit dislocations are observed in the Ag/Cu(111) system after deposition at RT and imaging at either 165 K [2] or RT [3], but not after deposition at 225 K and imaging at 170 K [2]. No systematic study of the temperature dependence of formation of misfit loops from the Moiré structure in either Au/Ni(111) or Ag/Cu(111) exist. It is therefore difficult to assess in advance, whether it will be possible to simulate the transition from the low temperature Moiré structure to the structure with misfit loops with ordinary MD simulations. It turns out that it is possible to observe formation of loops by MD simulations. Simulations of the Moiré structure in the $n_{Cu} = 9$ or 10 as well as of the 4 supercell system carried out at 800 K showed, in all cases, formation of misfit dislocations. It is also possible to observe the formation of misfit loops in simulations of compact Ag islands on wide Cu substrates. In one case a pseudomorphic Ag island consisting of 979 atoms was placed on a large Cu substrate (115×115 Å) and annealed to 800 K. The simulation shows that the island expands its internal lattice constant while maintaining the hexagonal (hetero–epitaxial) structure and that misfit dislocation loops form during the process. After just 1 ns of simulated time one 3–vacancy loop, four 4–vacancy loops, and one 5–vacancy loop have formed along with several adatoms and small islands ontop the overlayer. From these simulations a general perception of the evolution of the triangular superstructure emerged: First, the loops nucleate at positions where the overlayer atoms are close to energetically unfavorable atop sites. The nucleation involves creation of Ag adatoms by concerted motion of several atoms in the Ag overlayer as well as in the topmost Cu layer. The loops form initially as 2 vacancies in the topmost Cu layer and then grow into loops consisting of 3-6 vacancies. During the process the loops migrate as well. In the following, details of representative processes of each mode are given.

Nucleation. Based on the high temperature MD simulations it was possible to identify several nucleation mechanisms. The mechanisms divide into two classes: One where one or two Ag atom(s) is (are) expelled from the overlayer leaving a structure with a hole and adatom(s). Following the expulsion a 2–vacancy misfit loop forms

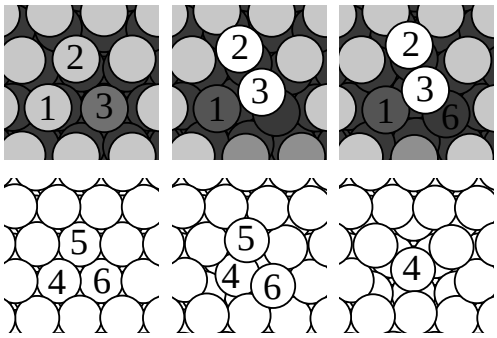

FIG. 1. Nucleation of a 2–vacancy misfit loop from the Moiré structure. The upper row shows a top view of the overlayer and the lower row shows the atoms below a cut–off between the overlayer and the topmost Cu layer. The columns are initial, transition and final states, respectively. The greyscale in the upper row roughly indicates the height of the atoms, with light atoms being highest.

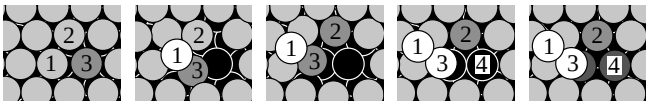

FIG. 2. Nucleation of a 2–vacancy misfit loop from the Moiré structure via an intermediate hole in the overlayer. Frames 1, 3, and 5 are local minimum energy configurations. Frames 2 and 4 are transition states.

in the topmost Cu layer by concerted motion of several atoms. The other class does not involve the intermediate hole/adatom stage. Instead Ag atoms are expelled while simultaneously dragging underlying Cu atoms along, thus forming the misfit loop without creating a hole in the overlayer.

An example of the 2nd class of nucleation is given in Fig. 1 which shows initial, transition, and final states for the process. The mechanism proceeds as follows: First the atop Ag atom (marked "3" in Fig. 1) and one of its neighbors (2) are expelled simultaneously from the overlayer while dragging the two underlying Cu atoms (5 and 6) along. The upward motion of atoms 5 and 6 allows Cu–atom 4 to shift from an fcc postion to a hcp position thus creating a 2-vacancy misfit loop surrounding that atom while atoms 2 and 3 form a Ag–dimer on the overlayer. The energy barrier for this mechanism is 1.00 eV.

For the other nucleation class, which involves hole formation, there are at least two possible ways the Ag atom can come up from the overlayer: One where the Ag atom moves up vertically and then settles in a hollow site at the surface. The other possibililty is an exchange where the atop Ag pushes one of its neighbors up onto the surface while taking this atom's place. One possibility of the latter mechanism is illustrated in Fig. 2. There are 2 transition states (frames 2 and 4) and 3 minima. The dark grey atop Ag atom pushes the atom to its left up onto

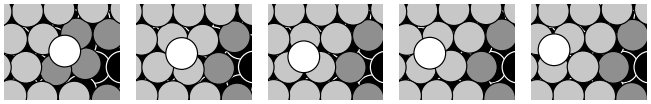

FIG. 3. Diffusion of the adtom formed in frame 3 of Fig. 2. Frames 1, 3, and 5 are local minimum energy configurations. Frames 2 and 4 are transition states.

the overlayer while taking this atom's place. Notice how the overlayer just below the adatom is distorted in the final configuration (frame 3) of this process: The adatom sits in what looks more like a skewed four–fold hollow site than a regular three–fold hollow site because of the broken symmetry. The energy barrier for this mechanism (frames 1-3) is 0.94 eV. Next, the former atop Ag atom and the two Cu atoms positioned below that Ag atom and below the hole come up from the Ag overlayer and the top Cu layer. This creates another adatom and a 2-vacancy misfit loop in the Cu layer in practically the same way as depicted in Fig. 1. Again at least two possibilities exist for the resulting adatom configuration. If the first adatom from the hole formation has not yet moved away from the region, it is possible that a dimer will form as shown here. Otherwise there will be two isolated adatoms after the loop formation. The barrier for the loop formation shown in frames 3-5 of Fig. 2 is 0.54 eV. Several other proceses resulting in a 2–vacancy loop which only differ in their details, e.g., the configuration of the adatoms, have been investigated, and all have very similar activation energies. The hole formation via exhange as in Fig. 2 was found to be marginally preferred to the mechanism where the atop Ag comes up vertically and settles in a hollow site. For the latter mechanism the lowest barrier obtained was 0.99 eV.

It is important to realize that the loop–configurations described thus far have a higher total energy than the Moiré structure. Hence, the configurations are not in a thermodynamical equilibrium, though entropic effects might play a role. The energy barriers for annihilation of the loops and returning to the Moiré structure are very low (~ 0.1 eV) compared to the barriers for formation of the loops. However, the loops can only disappear if the adatoms remain in the vicinty of the loop, or, in other words, if the energy barriers for adatom diffusion away from the loop are higher than the barriers for annihilation of the loops. In fact, the barries for diffusion on the overlayer can be lower than the barriers for annihilation. The adatom formed in frame 3 of Fig. 2 can easily diffuse away from the hole region. In the experimental situation adatoms will probably diffuse to step edges which are not present in the simulations. One possible diffusion path is shown in Fig. 3. The adatom diffuses from the skewed four–fold site close to the hole to a three–fold hollow site further into the overlayer. There are 2 transition states (frames 2 and 4) and 3 minima.

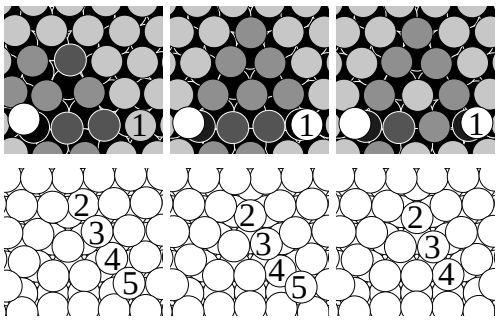

FIG. 4. Growth of a 3–vacancy loop into a 4–vacancy loop: Initial, transition and final states.

The highest barrier is from frame no. 1 to frame no. 3, 106 meV. The barrier for the transition from frame no. 3 to frame no. 5 is only 10 meV. For the mechanism shown in Fig. 2 the barrier for annihilation of the loop, i.e., the barrier for going "backwards" from frame 3 to 1 in Fig. 2, is 127 meV. Hence, it is possible for a single adatom to escape from the hole region. For the mechanism shown in Fig. 1 the situation is not so favorable. The barrier for annihilation is in this case 54 meV. Other configurations of the dimer give slightly higher annihilation energies ($\simeq 90$ meV) but the barrieres for escape of the dimer (or splitting of the dimer) are still higher. A 2–vacancy loop with no adatoms in its vicinity can annihilate too, leaving a structure with 2 missing atoms in an otherwise locally perfect overlayer and no vacancies in the substrate. The energy barrier for such an annihilation is 0.25 eV with the final configuration being 65 meV higher in energy. Based on these results it can be concluded that the most probable scenario for loop nucleation is via hole formation and subsequent diffusion of the adatoms to step edges.

Growth. Once a 2–vacancy loop exists it can increase in size by one vacancy by expelling another atom. Figure 4 shows an example of growth of a 3–vacancy loop into a 4–vacancy loop. Atoms 1 and 5 come up simultaneously thereby enabling atoms 2, 3, and 4 to shift from fcc to hcp positions. After the growth event atom 1 has become an adatom and atom 5 has taken its place. The energy barrier is 0.56 eV. Several growth events which proceed similarily to the one in Fig. 4 were observed in the simulations. Misfit loops as large as 6 vacancies were observed. In all investigated cases the energy barriers were in the range $0.32 - 0.71$ eV depending on the details of the configurations. Hence, it can be concluded that nucleation controls the loop formation. Once the loops have formed at a sufficiently high temperature, growth proceeds rapidly.

Motion. During the growth mode it is observed that loops migrate. Figure 5 shows migration of a 3–vacancy loop. The top row shows the surface while the bottom row shows how the atoms in the topmost substrate layer

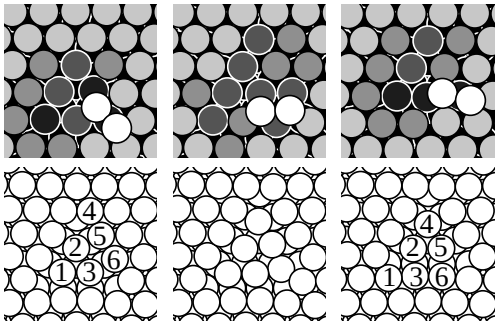

FIG. 5. Motion of a 3–vacancy loop. Initial, transition, and final states.

rearrange to accomplish motion of the loop by 1 nearest neighbor distance. In the initial state the loop surrounds the cluster of atoms 1, 2, and 3, and in the final state the loop surrounds atoms 2, 4, and 5. The energy barrier for this process is 0.54 eV. A loop can also migrate by a partial annihilation. In that case an adatom situated close to the loop reenters the overlayer thereby decreasing the loop size by one. Subsequently another atom can be squeezed out. In this way the loop moves one spacing via a smaller intermediate configuration.

Since no systematic annealing studies of the Moiré structure exist, it is difficult to compare the activation energies obtained in this work with experimental results. With the activation energy for formation of a 2–vacancy misfit loop of 0.94 eV and assuming a preexponential factor of $5\times10^{12}\,\mathrm{s}^{-1}$, the rates from an usual harmonic transition state expression become $8\times10^{-4}\,\mathrm{s}^{-1}$ and $7\,\mathrm{s}^{-1}$ at 300 K and 400 K, respectively. Hence, the simulations seem to be in reasonable agreement with the experimental observations considering that kinetic effects might be responsible for the formation of misfit loops after Ag deposition at RT. Also, in the Au/Ni(111) system, which exhibits very analogous behavior to the Ag/Cu(111) system, the Moiré structure had to be annealed to 400 K before the misfit loops formed [1]. The EMT potentials applied in this work have successfully been fit to properties such as elastic constants, stacking–fault energies and vacancy formation energies. However, it is well know that effective–medium–like potentials (EMT or EAM) in some cases have difficulties in reproducing accurate results for systems with low coordinated atoms, e.g., adatom diffusion. The diffusion barrier for Ag on Ag(111) with the present EMT parameterization (0.06 eV) is in perfect agreement with other EMT or EAM potentials, while experiment and *ab initio* calculations give barriers $\simeq 0.1$ eV [11]. The results presented here are likely to suffer from the low coordination problem as well thus putting a limitation on the absolute accuracy of the activation energies. A decrease of the nucleation activation energy to, say, 0.8 eV would increase the rate of loop formation at $T = 300$ K by three orders of magnitude. The effect of the substrate thickness was investigated by performing some of the NEB simulations with 3 static and 10 dynamic substrate layers as well as with just 4 dynamic layers. The effect is negligible: The energy barriers were reduced by 1 %. Finally, it should be mentioned that the interpretation [2] of experimental STM results in terms of Vegard's law indicates that no Cu is alloyed into the Ag overlayer in contrast to the situation for Au/Ni(111) [1]. In the simulations presented here, Cu is indeed alloyed into the overlayer. It is hard to imagine loop formation mechanisms which would not involve such alloying as an intermediate stage. Perhaps the alloyed Cu could exchange with Ag adatoms and move to step edges, but no evidence of this was observed in the simulations.

The present work was supported by the US Department of Energy under contract no. W-7405-ENG-36.

[1] J. Jacobsen *et al.*, Phys. Rev. Lett. **75**, 489 (1995).
[2] F. Besenbacher, L. P. Nielsen, and P. T. Sprunger, Chap. 6 in *Growth and Properties of Ultrathin Epitaxial Layers* eds. D. A. King and D. P .Woodruff, Elsevier (1997).
[3] B. Aufray *et al.*, Microsc. Microanal. Microstruct. **8**, 167 (1997).
[4] I. Meunier *et al.*, Phys. Rev. B **59**, 10910 (1999).
[5] S. Heinze *et al.*, Phys. Rev. Lett. **83**, 4808 (1999).
[6] K. W. Jacobsen, J. K. Nørskov, and M. J. Puska, Phys. Rev. B **35**, 7423 (1987).
[7] K. W. Jacobsen, P. Stoltze, and J. K. Nørskov, Surf. Sci. **366**, 394 (1996).
[8] The EMT implementation follows that given in [7,10], but the parameterization differs slightly. The parameters used in this work have been fit to elastic constants, relaxed vacancy formation energies, relaxed intrinsic stacking–fault energies, and heats of solution for Ag in Cu and Cu in Ag. The parameters following the notation in Ref. [7] are (Ag;Cu): s_0: (3.01;2.67), E_0: (-2.96;-3.51), V_0: (2.679;3.010), η_2: (1.400;1.494), κ: (2.365,2.500), λ: (1.956;1.942), n_0: (0.0059;0.0068).
[9] H. Jónsson, G. Mills, and K. W. Jacobsen, Chap. 16 in *Classical and Quantum Dynamics in Condensed Phase Simulations* eds. B. J. Berne *et al.*, World Scientific (1998).
[10] P. Stoltze, *Simulation methods in atomic–scale materials physics*, Polyteknisk Forlag (1997).
[11] J. J. Mortensen *et al.*, Springer Ser. Sol. State Sci. eds. A. Okiji *et al.*, **121**, 173 (1996).
[12] C. Kittel, *Introduction to Solid State Physics*, 4th. ed. (Wiley, New York, 1971).
[13] J. Hartford *et al.*, Phys. Rev. B **58**, 2487 (1998).
[14] L. Vitos *et al.*, Surf. Sci. **411**, 186 (1998).
[15] P. A. Korzhavyi *et al.*, Phys. Rev. B **59**, 11693 (1999), and references therein.
[16] F. R. de Boor *et al.*, *Cohesion in Metals: Transition Metal Alloys*, (North Holland, 1988).